Journal of Engineering and Computer Sciences
Vol. 16, No. 1, pp.59-70 (Jan 2024)

# Effect of the Aspect Ratio on the Buckling Load of Unidirectional Carbon Fiber Reinforced Composites

**Mansour Alturki**
Department of Civil Engineering, College of Engineering, Qassim University, Buraydah 51452, Saudi Arabia. Email: m.alturki@qu.edu.sa

**A. E. Abdelraheim**
Department of Mechanical Engineering, College of Engineering, Qassim University, Buraydah 51452, Saudi Arabia. Email: aahmad@qu.edu.sa

[Received: 4 March 2025, Revised: 17 March 2025, Accepted: 20 March 2025, Published 11 May 2025]

***Abstract*:** Elastic instabilities, such as buckling and snapping-through, serve as key mechanisms in metamaterials and periodic structures designed for self-centering, energy absorption, and dissipation. These systems rely on single or multiple buckling events of interconnected axially compressed elements. A promising candidate material for such elements is the unidirectional carbon fiber-reinforced composites, provided that elastic buckling precedes inelastic damage failure. This study presents a numerical investigation to examine the failure stress of unidirectional carbon fiber-reinforced composites with various aspect ratios (AR). Finite element analyses were performed on tested specimens of unidirectional carbon fiber-reinforced polymer composites found in the literature. Results indicate that a minimum AR of 28 is required to induce buckling failure rather than other modes, with Euler's equation sufficiently predicting critical buckling stress in this range. On the other hand, for AR values between 15 and 28, compression-shear or shear failure becomes dominant, while AR below 15 typically results in compression failure. Accounting for shear correction and material nonlinearity enables precise prediction of critical buckling stress across all AR.

***Keywords*:** Buckling; carbon fibre; elastic instabilities; energy dissipation; composite

## 1. INTRODUCTION

Modern seismic design aims to dissipate induced seismic energy through controlled inelastic deformations at predefined locations that are called plastic hinges, ensuring collapse prevention. While effective for life safety criteria, structures subjected to such deformations often sustain severe residual damage, requiring costly repairs or becoming unusable, such as concrete structures [1]. To address this issue, a new objective prioritizes eliminating inelastic deformations by utilizing elastic self-centering and energy dissipation devices, which exploit nonlinear elastic instabilities (e.g., buckling-restrained systems) to dissipate energy without permanent deformation [2,3]. An illustrative example of the use of this concept is shown in Figure 1.

Elastic buckling and snapping-through of struts, thin plates, and shells serve as key mechanisms in metamaterials and periodic structures designed for self-centering, elastic energy absorption, and dissipation. These structures undergo relatively high overall shortening upon compressive loading and then they regain their original shape upon loading removal. Such structures depend on single or progressive buckling events of interconnected axially compressed elements [4]. Examples of such systems include shape-reconfigurable and energy dissipating systems comprising of arrays of tilted and inclined beams [5–10], sinusoidally curved beams [11–13], and three-dimensional periodic structures [14–16].

There are many possible ways to achieve nonlinear elastic response using controlled instabilities of single elements or systems. In such elements, a compressive axial load is applied to the structure causing the structure to buckle in multiple buckling modes before undergoing inelastic deformations. This could be achieved by continuously constraining the lateral deformations and forcing the system to respond in higher buckling modes before reaching material strength. This allows the structure to deform and overly shorten in a nonlinear elastic manner and with a higher rate when higher buckling modes are exited [17]. An example of this system is a steel rod or plate constrained by a tube as shown in Figure 2.

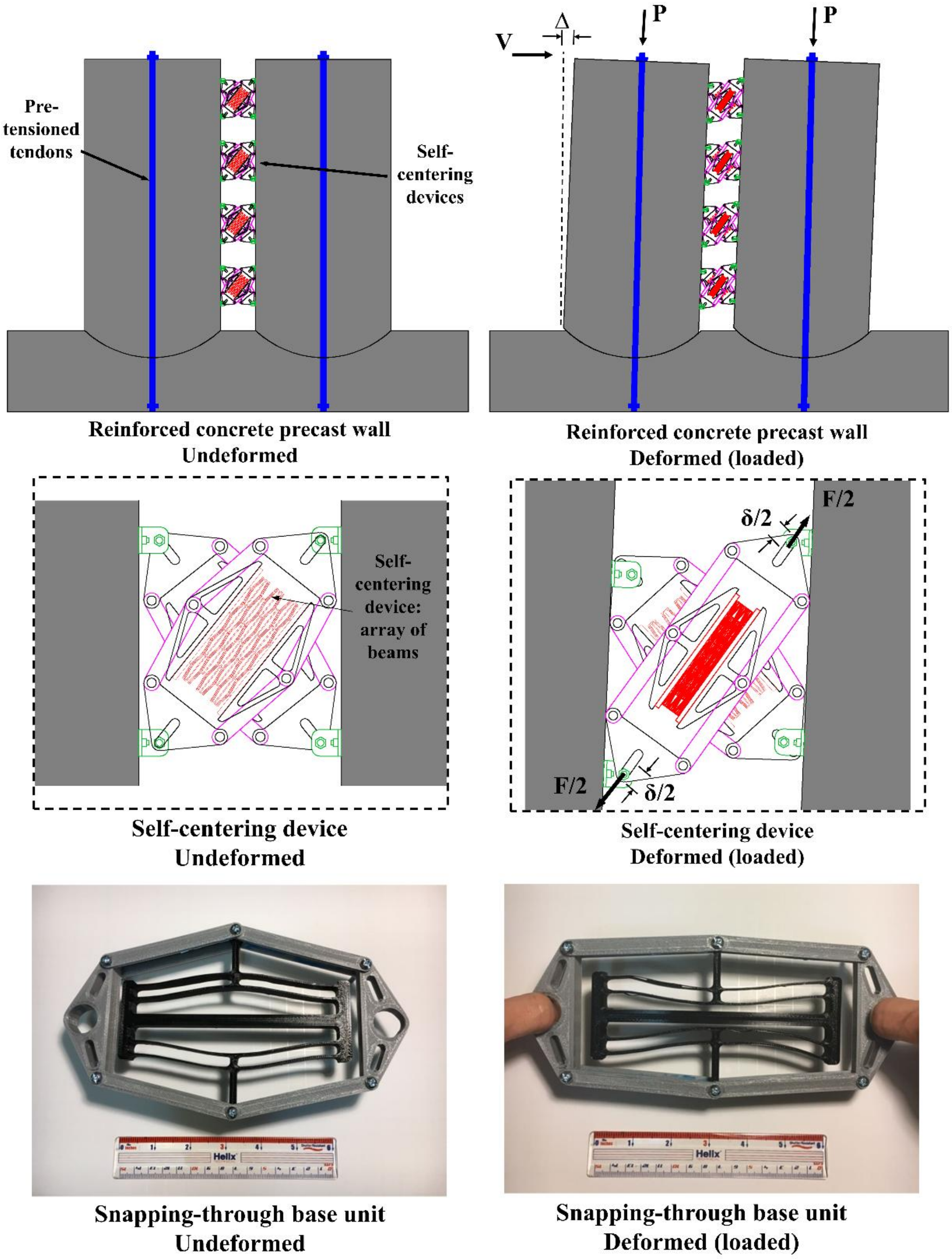


Figure 1: Illustration of using self-centering and energy dissipation devices for seismic protection

A possible material to be used in such structures is unidirectional carbon fiber reinforced composites provided that elastic buckling will occur before inelastic damage. Unidirectional carbon fiber reinforced composites are materials of interest to be utilized under compression since their behavior and failure could be controlled (to a certain extent) more than conventional construction materials Also, since they have high proportional limit stress (ultimate stress) and lower elastic stiffness, and hence low buckling length [18].

The main question considered here is at what aspect ratio a compression failure will be avoided and buckling event will be achieved. In this study, nonlinear and finite element analyses (FEA) are carried out on tested unidirectional carbon fiber reinforced struts found in the literature. The nonlinear and FEA are combined with a numerical study to predict the buckling load, failure stresses, and failure modes of struts with various aspect ratios. This study will help to determine the proper dimensions of buckling elements based on critical buckling stress and aspect ratio.

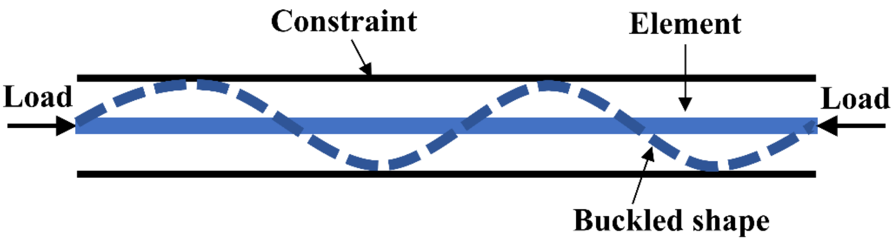

Figure 2: Illustration of multiple buckling events of a constrained rod/plate under compression

Struts with rectangular sections are examined. The struts have unidirectional carbon fibers in the direction of loading (the longitudinal direction). The applied loads are only axial loads as shown in Figure 3. However, when the element starts buckling, bending moments and shear forces are developed along its axis (second-order effects). These forces and moments create tensile, compressive, and shear stresses within the fibers and the matrix of the composite element. The failure of such an element depends on the ratios of these stresses to each other. These ratios are controlled by the aspect ratio (*AR*) defined as the height-to-thickness ratio or $AR = h / t$, where $h$ is the height of the strut and $t$ is the thickness as illustrated in Figure 3. Therefore, this study focuses on examining this parameter and aiming to determine key values (or ranges) for *AR* at which a failure type would transition to another one. At these key values, buckling stresses and failure modes with the *AR* ratio are studied. This characteristic is of great significance for the design of structured periodic material to ensure a specific progressive snap-buckling events are archived before compression failure.

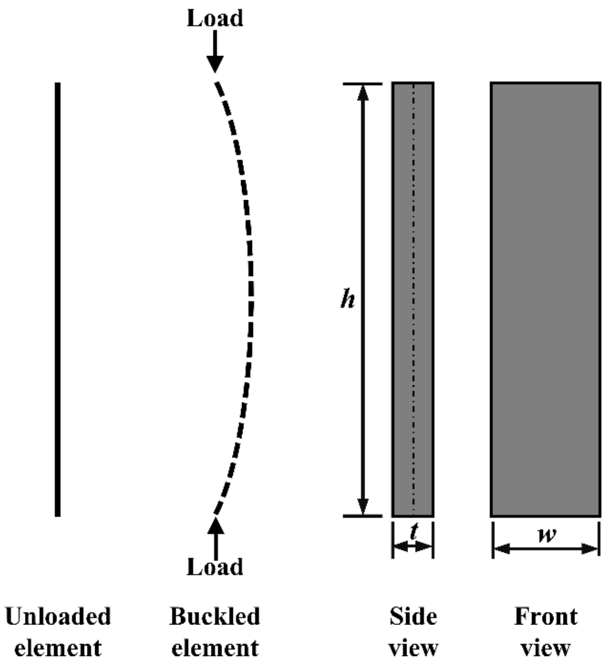

Figure 3: Schematic for axially loaded strut and its buckled shape

# 2. LITERATURE REVIEW

## 2.1 Failure of Unidirectional Laminates under Compressive Loading

The prediction of the behavior and failure mechanism of unidirectional laminates under compressive loading depends on many factors including geometric factors, material nonlinearity, and shear deformation. Therefore, they have complex behavior and various failure modes. Their use in applications depends mainly on experimental tests since the uncertainties of predicting the response are high even for simple elements and structures [19].

In general, thin composite plates and struts with high slenderness under compressive loadings usually buckle and their buckling stress can be predicted reasonably well assuming that the material is linear elastic. However, plates with low slenderness usually fail at relatively high compressive stresses and hence it is essential to take account of the nonlinear material behavior in the fiber direction along with shear effects [20].

The importance of material nonlinearity and shear effects on buckling loads of unidirectional laminates has been recognized in the literature. It has been concluded that the Euler buckling load can be significantly reduced due to the presence of bending and transverse shear deformation, especially for plates with low slenderness [21]. Unidirectional fiber-reinforced laminates exhibit significant nonlinear behavior along the fiber direction, progressively losing stiffness with increasing compressive strain level [19].

## 2.2 Determinations of Buckling Loads

There are a few approaches to determine the buckling load of compressed unidirectional fiber-reinforced composite. These approaches are relatively simple because (a) the examined elements here have fibers in one direction (orientation), (b) the fibers are in the direction of loading, (c) the elements are not supported (free) in the long directions, and d) the longitudinal modulus of elasticity can be sufficiently determined based on the rule of mixtures.

The buckling analysis of such elements depends on several factors as follows:

1. The value of the aspect ratio (*AR*) about the weak direction.
2. Shear deformation, which has an important role in the buckling load since the shear modulus of unidirectional laminates (*G*) is relatively low and hence low shear stiffness. The ratio of the elasticity modulus (*E*) of unidirectional carbon fiber-reinforced laminates to *G* is about 25 [18].
3. The nonlinearity of the stress-strain curve of unidirectional carbon fiber reinforced laminates under compression.

## 2.3 Analytical Buckling Analysis

For a compressed strut, the critical buckling stress can be determined from the Euler critical buckling load ($P_{cr}$) as follows:

$$P_{cr} = \frac{\pi^2 E\, I}{(k\, h)^2} \tag{1}$$

where $k$ is the end conditions factor ($k = 0.5$ for fixed end conditions used in this study), and $I$ is the cross-section moment of inertia around the weak direction. The latter may be calculated as:

$$I = \frac{w\, t^3}{12} \tag{2}$$

where $w$ is the strut width. If $A$ was considered as the sectional area (i.e. $A = w\, t$); the critical buckling stress may be calculated as:

$$\sigma_{cr} = \frac{P_{cr}}{A} \tag{3}$$

It should be mentioned that the critical buckling stress is independent (see factors listed above) of the strut width and it only depends (geometrically) on *h* and *t*. This can be seen when substituting Eqs. (2) and (3) into Eq. (1) which yields the following expression for the critical buckling stress ($\sigma_{cr}$):

$$\sigma_{cr} = \frac{\pi^2 E\, t^2}{3\, h^2} \tag{4}$$

The expression in Eq. (4) neglects the shear deformation; however, for carbon laminates, shear deformations should be included as discussed earlier. Using the expression developed in [22], the critical buckling stress is corrected for shear ($\sigma_{crs}$) as follows:

$$\sigma_{crs} = \frac{\sigma_{cr}}{1 + 1.2\frac{\sigma_{cr}}{G}} \tag{5}$$

2.4 Non-linear Buckling Analysis

To take into account the nonlinearity of the stress-strain curve, *E* in the expression of Eq. (4) is replaced by the tangent modulus of elasticity ($E_t$) which is a function of the applied strain. Therefore, $\sigma_{cr}$ is determined iteratively. $E_t$ is determined as follows:

$$E_t(\varepsilon) = \sigma'(\varepsilon) \tag{6}$$

where the stress-strain equation can be taken from the stress-strain curve based on the curve fitting proposed in [19] as follows:

$$\sigma(\varepsilon) = 1261\,\varepsilon - 118.1\,\varepsilon^2 - 19.39\,\varepsilon^3 \tag{7}$$

For the iterative expression (nonlinear) in Eq. (6), Full Newton-Raphson method with three equal steps [23] was used to determine the buckling stress. Out-of-balance stress ($g$) of less than 0.001 was used as an indication to move to the next iteration. Four to five increments per step were required to meet the condition for $g$.

## 3. METHODS

The main focus of this study is to determine the critical buckling stresses of unidirectional fiber-reinforced struts in relation with the *AR*. Thus, the main objective is to know at what *AR* a composite strut will buckle instead of failing on other failure modes. This could be studied based on the *AR* of a strut by relating it with proportional limit stress ($\sigma_p$) to the critical buckling stress. $\sigma_p$ is defined as the highest stress at which stress is directly proportional to strain. For steel, this stress is the yield stress, while for unidirectional fiber-reinforced composites is the ultimate stress. From the expression in Eq. (4), *AR* is determined in terms of $\sigma_p$ as:

$$AR = h/t = \pi\sqrt{\frac{E}{3\,\sigma_p}} \tag{8}$$

This expression, however, does not consider the effects of shear deformation or nonlinearity of the material.

### 3.1 FE Modeling and Analysis

Finite element analyses (FEA) were conducted using ABAQUS software [24] to perform buckling load analysis on strut models with geometric and material properties as listed in Table 1. The model has fixed edges along the two width edges with free translation in the x-axis direction at one of the edges where the loading is applied, as shown in Figure 4(a). A linearly distributed load was applied on the edge to ensure uniformity. The buckling load is then determined as the edge load multiplied by the width (*w*). The struts have piles layups of 16-ply with 0.125 mm thick as shown in Figure 4(b). The struts were modeled as shell structures using linear elastic laminate material properties, meshed with four-node shell elements (S4). The mesh size was determined through a refinement study to ensure accuracy. Large deformations were considered by including geometric nonlinearity in the analyses. The mesh used to discretize the element is also shown in Figure 4(c). Nonuniform mesh discretization was used to induce buckling. The resulted values from FEA from this and the previous sections with test results are plotted against *AR*.

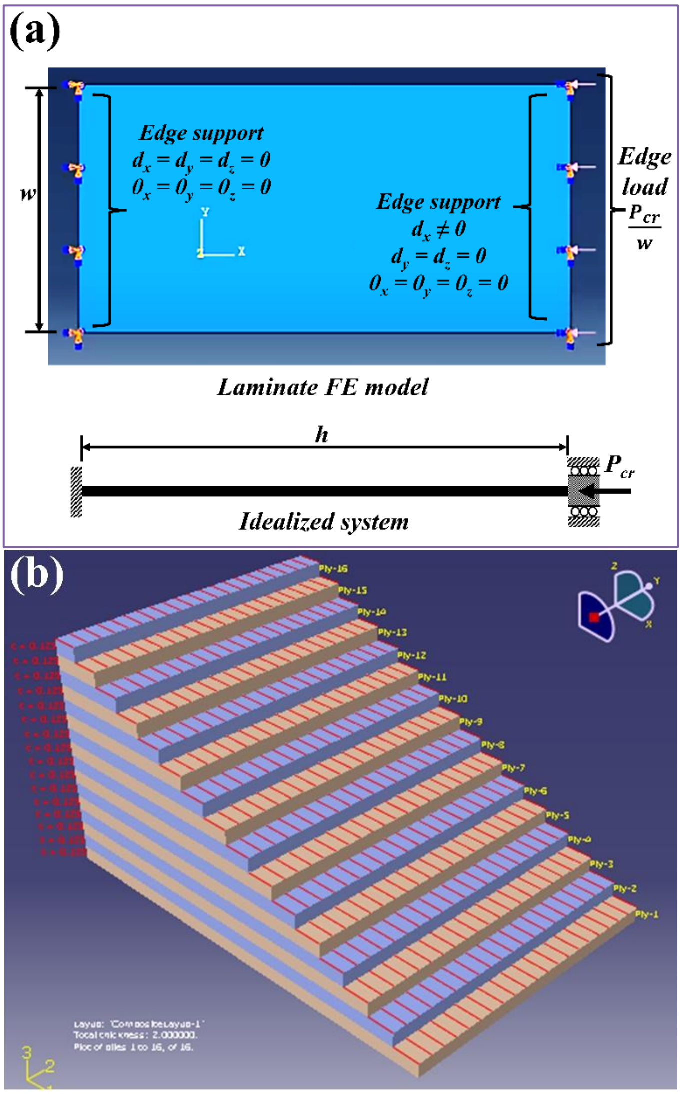

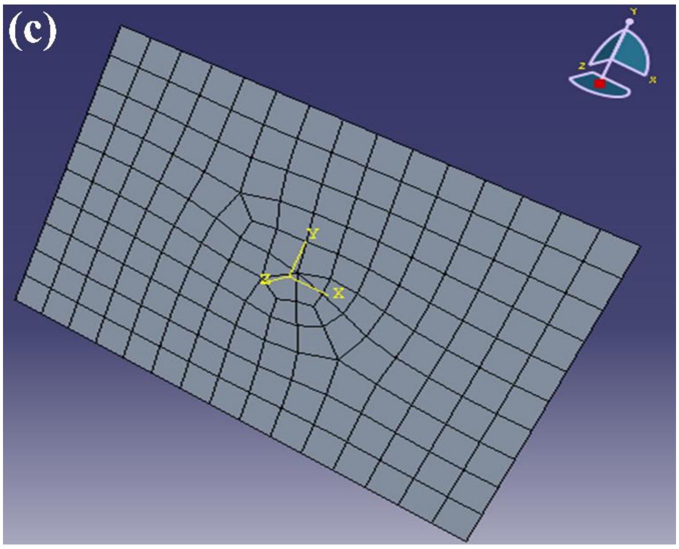


Figure 4: FE model of the struts: (a) model loading and boundary conditions, (b) piles layups, and (c) mesh discretization for the strut

Table 1: Properties values of the unidirectional carbon fiber reinforced struts

| Property | Value |
|---|---|
| Type | Unidirectional carbon fiber/epoxy reinforced |
| Sectional dimensions: *w* by *t* (see Figure 3) | 10 mm by 2 mm |
| Height, *h* (see Figure 3) | 10 mm to 100 mm |
| Longitudinal elastic modulus in the direction of the fibers, $E_L$ | 120 GPa |
| Transverse elastic modulus to the direction of the fibers, $E_T$ | 10 GPa |
| Shear modulus, *G* | 5 GPa |
| Poisson's ratio, $\upsilon$ | 0.34 |
| Breaking strength of the fibers in tension, $S_L^+$ | 1600 MPa |
| Breaking strength of the fibers in compression, $S_L^-$ | 1600 MPa |
| Breaking strength of the epoxy in tension, $S_T^+$ | 60 MPa |
| Breaking strength of the epoxy in compression, $S_T^-$ | 260 MPa |
| Shear strength, $S_{LT}$ | 90 MPa |

### 3.2 Experimental Validation

Finite element analysis was also performed on tested unidirectional carbon fiber-reinforced struts reported in [19] to determine the buckling stresses. The tested struts have geometric and material properties as listed in Table 1 but with selected heights of 15, 30, and 50 mm. The selection of these height values was made to examine the possible failure modes (compression, compression-shear, and buckling). The analyses were performed to check the FEM model and results before continuing with other study cases that are not reported in the literature. The simulated cases and other results are used to compare with the analytical and the nonlinear buckling analyses to draw a conclusion about the relation between buckling failure and *AR*.

The critical buckling stress was determined by dividing the buckling load per the width by the strut thickness (2 mm). For the 15 mm and 50 mm long struts shown in Figure 5, the critical buckling stress $\sigma_{cr}$ is 1669.1 and 480.6 MPa, respectively.

Table 2 presents the critical buckling stress from the FEA compared with reported test results. The error percentage between the two values indicates a reduction in the difference with an increase in length or *AR* as shown in Figure 6.

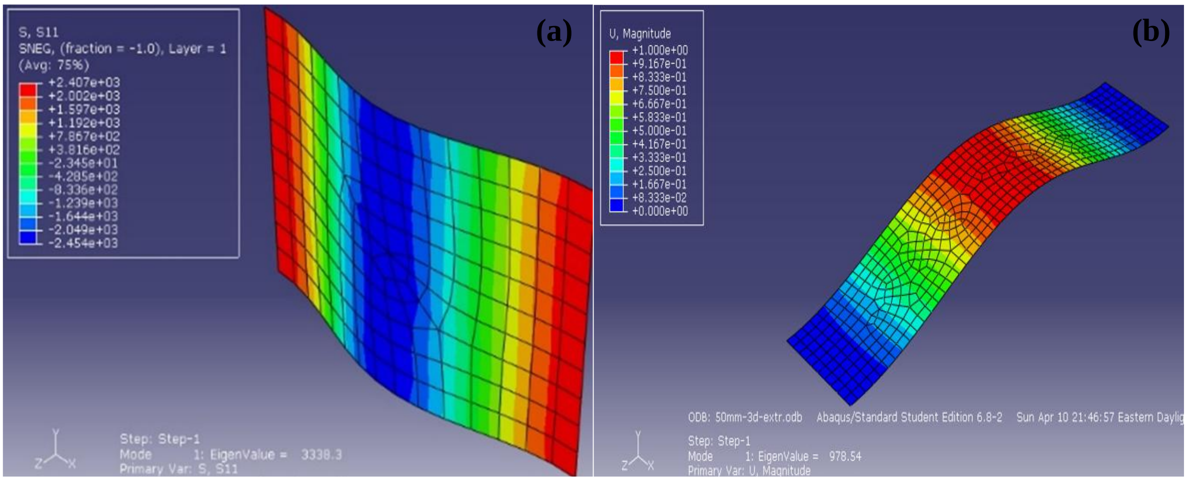

Figure 5 Buckling analysis results for struts heights of (a) 15 mm, and (b) 50 mm

**Table 2:** Results from FEA compared with reported test results

| Strut length | 15 mm | 30 mm | 50 mm |
|---|---|---|---|
| **Test result** | 1530.0 MPa | 911.7 MPa | 490.9 MPa |
| **FEA result** | 1669.1 MPa | 975.5 MPa | 480.6 MPa |
| **Error** | 9.1 % | 7.0 % | 2.2 % |

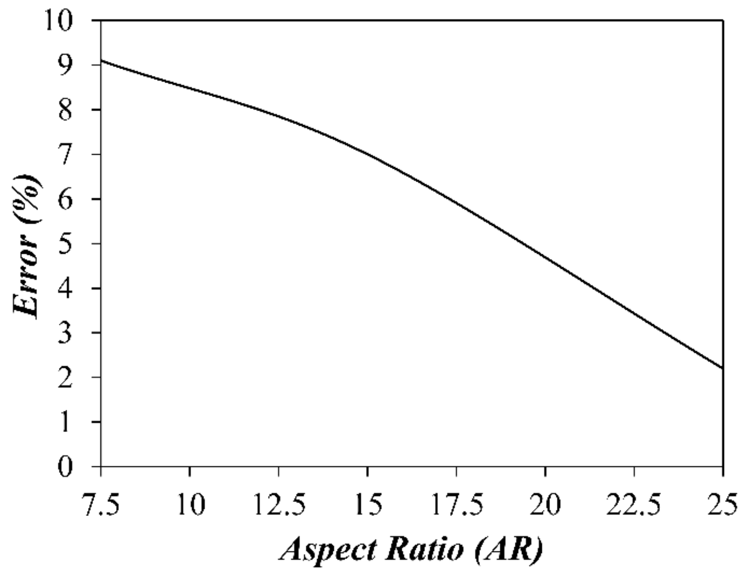

Figure 6: Error percentage between FEA results and reported test results versus *AR*

## 4. RESULTS AND DISCUSSIONS

The resulted buckling stress values from FEA for the properties listed in Table 1 are plotted against *AR* as shown in Figure 7. The figure also includes the curves based on Eq. (4) to Eq. (6) and the test results reported in [4]. Based on Figure 7, it can be noticed that the actual buckling stress is much smaller than that of the Euler buckling stress, especially for an AR of 20 or less. The shear correction and the inclusion of nonlinearity effects are important to represent the actual behavior of a compressed strut. Their effects are more pronounced for an AR of 20 or less (Figure 7). The inclusion of nonlinear material properties is important for struts with low AR (< 12). For struts with high AR (> 28), any method will result in an accurate estimate of the buckling stress as can be seen in Figure 7. This means the buckling stress is mainly dependent on the Euler buckling stress (only at this range) while shear deformation and the nonlinearity have no notable effects. Figure 7 can be divided into 3 regions where a probable failure mode will occur: (a) for AR < 15, compression failure, (b) for 15 < AR < 28, compression-shear or shear failure, and (c) for AR > 28, buckling. Shear correction and the inclusion of nonlinearity in calculating the critical buckling stress agree with FEA and experimental results. Therefore, they are sufficient to predict critical buckling stress at any AR. Nonetheless, FEA seems to overestimate critical buckling stress for struts with low AR.

A notable discrepancy of approximately 9.1% is observed between the compressive failure stress of the experimentally tested strut with height of 15 mm (*AR* = 7.5) and the corresponding FEA result, as indicated in Table 2 and shown in Figure 7. This difference is attributed to two primary factors: (1) very low *AR*, which amplifies the influence of material nonlinearity and shear deformation, and (2) inherent deviations in experimental testing conditions and dimensional variations in test specimens.

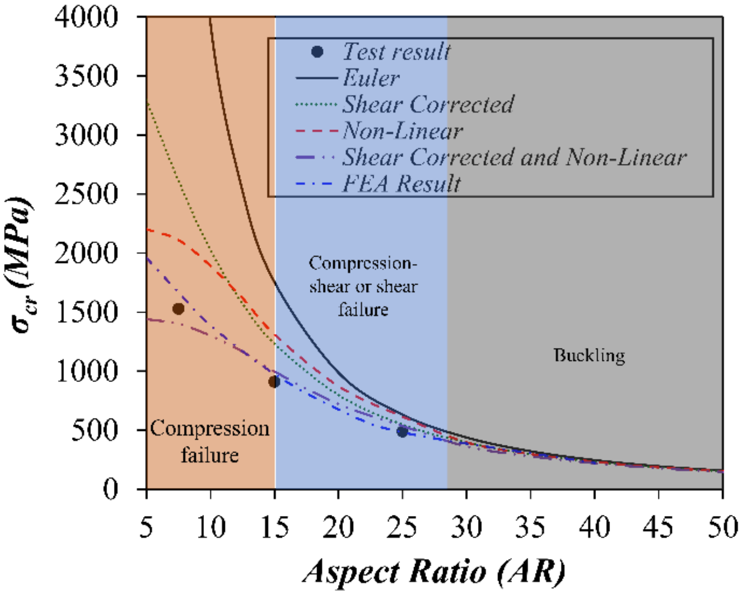


Figure 7: Comparison of critical buckling stress of different approaches with test and FEA results versus AR

To answer the main question of the study, which is at what *AR* a unidirectional carbon fiber reinforced strut will buckle instead of failing on other failure modes, struts with a minimum *AR* of 28 should be used. This (based on this study) will ensure a buckling event before any other failure mode. Although it was previously concluded that an *AR* of 18.5 is the minimum required to achieve buckling, this value is theoretical. It should be mentioned that these results and conclusions are for struts with fixed-end conditions.

Compared to steel, unidirectional carbon fiber reinforced struts are more suitable to achieve buckling since they have high proportional limit stress (ultimate stress) and low elastic stiffness, and hence low buckling length (or *AR*). A compression illustrating this advantage compared to steel is presented in Table 3.

Table 3: Compression between unidirectional carbon fiber and steel minimum required buckling ratios

| Material | $E$ | $\sigma_p$ | *AR* from Eq. (8) |
|---|---|---|---|
| **Steel** | 200 GPa | 250 MPa | 51.3 or higher |
| **Unidirectional carbon fiber-reinforced struts** | 120 GPa | 1600 MPa | 15.7 to 28 |

For the properties given in Table 3, the minimum theoretical height for the strut to avoid compression failure is 31.5 mm or an AR of 15.7. If the stress $\sigma_p$ is modified for shear deformations using Eq. (5), the minimum theoretical height to avoid compression and shear failures is 37.0 mm or AR of 18.5 (18 % increase). Therefore, to ensure buckling behavior (desired) for a strut with a rectangular section and fixed at both ends, a minimum AR of 18.5 must be used. The value 28 for *AR* serves as practical limit at which buckling is always guaranteed for unidirectional carbon reinforced fiber laminates.

## 5. CONCLUSION

This presented study utilized finite element analysis to numerically investigate the critical buckling stress of unidirectional carbon fiber-reinforced polymer struts, focusing on the influence of aspect ratio on their failure mechanisms and load-bearing performance. Based on the analysis results and the comparison between the different methods of analysis used to determine the critical buckling stress, the following points can be stated:

1. A minimum AR of 28 is required to achieve buckling and avoid other failure modes. For this range, using the Euler equation [Eq. (3)] to predict the critical buckling stress is sufficient.
2. Struts with 15 < AR < 28 will probably have compression-shear or shear failure.
3. Struts with AR < 15 will probably have compression failure.
4. For unidirectional carbon fiber reinforced struts with factors listed in Section 2, the inclusion of shear correction and nonlinearity effects is sufficient to predict critical buckling stress at any AR.
5. FEA for critical buckling stress agrees with the experimental result and the analytical buckling analysis.
6. Although the strut width *w* was theoretically shown to not affect critical buckling stress, it may have one for struts with low *AR* since the increase in the sectional area increases the strut's compressive axial resistance.
7. Shear deformations and failure could be reduced if other types of fiber orientations are used. Such as the use of a combination of unidirectional and stitched (confining) fibers.

While this study establishes a relationship between aspect ratio (*AR*) and buckling load in unidirectional carbon fiber-reinforced composites, several unresolved questions and opportunities for further investigation remain. To advance the practical application of these findings, particularly in seismic protection systems, future work should address the following:

1. Although the conclusion here is that struts with AR of 28 or higher can achieve buckling, the behavior under repeated and dynamic loads must be studied to be safely used in self-centering devices for seismic protection.
2. Although the strut width (*w*) was theoretically shown to not influence critical buckling stress, it may have one for struts with low *AR* since the increase in the sectional area increases the struts compressive axial resistance.
3. Shear deformations and failure could be reduced if other types of fiber orientations are used. Such as the use of a combination of unidirectional and stitched (confining) fibers.

**Acknowledgments**

The Researchers would like to thank the Deanship of Graduate Studies and Scientific Research at Qassim University for financial support (QU-APC-2025).

## REFERENCES


[1] M.J.N. Priestley, Performance based seismic design, in: 12th World Conference on Earthquake Engineering, New Zealand Society for Earthquake Engineering, Upper Hutt, New Zealand, 2000: p. 2831.

[2] J.B. Mander, C.T. Cheng, Seismic resistance of bridge piers based on damage avoidance design, National Center for Earthquake Engineering Research, Buffalo, NY, 1997.

[3] M. Alturki, R. Burgueño, Equivalent viscous damping for system with energy dissipation via elastic instabilities, Eng Struct In review (n.d.).

[4] N. Hu, R. Burgueño, Buckling-induced smart applications: recent advances and trends, Smart Mater Struct 24 (2015) 063001. https://doi.org/10.1088/0964-1726/24/6/063001.

[5] B. Haghpanah, A. Shirazi, L. Salari-Sharif, A. Guell Izard, L. Valdevit, Elastic architected materials with extreme damping capacity, Extreme Mech Lett 17 (2017) 56–61. https://doi.org/10.1016/j.eml.2017.09.014.

[6] M. Jin, X. Hou, W. Zhao, Z. Deng, Reusable energy-absorbers design harnessing snapping-through buckling of tailored multistable architected materials, Smart Mater Struct 33 (2024) 065012. https://doi.org/10.1088/1361-665X/ad46a3.

[7] C.S. Ha, R.S. Lakes, M.E. Plesha, Design, fabrication, and analysis of lattice exhibiting energy absorption via snap-through behavior, Mater Des 141 (2018) 426–437. https://doi.org/10.1016/j.matdes.2017.12.050.

[8] S. Liu, A.I. Azad, R. Burgueño, Architected materials for tailorable shear behavior with energy dissipation, Extreme Mech Lett 28 (2019) 1–7. https://doi.org/https://doi.org/10.1016/j.eml.2019.01.010.

[9] Z. Zhang, Z.D. Xu, Light-weighted quasi-zero stiffness device based on connected inclined beams on a flexible support, Journal of Low Frequency Noise Vibration and Active Control (2024). https://doi.org/10.1177/14613484241300749.

[10] X. Yao, H. Zhao, R. Ma, N. Hu, Manipulating localized geometric characteristics in multistable energy-absorbing architected materials, Thin-Walled Structures 205 (2024) 112535. https://doi.org/10.1016/J.TWS.2024.112535.

[11] D.M. Correa, T. Klatt, S. Cortes, M. Haberman, D. Kovar, C. Seepersad, Negative stiffness honeycombs for recoverable shock isolation, Rapid Prototyp J 21 (2015) 193–200. https://doi.org/10.1108/RPJ-12-2014-0182.

[12] C. Zhou, F. Zhang, X. Zhang, Y. Chen, Hierarchical negative stiffness structures with improved resilience and energy absorption capability, Mater Today Commun 42 (2025) 111371. https://doi.org/10.1016/J.MTCOMM.2024.111371.

[13] J. Hua, Y. Zhou, Z. Meng, C.Q. Chen, Pre-compressed beam-based multistable mechanical metamaterials with programmable loading and unloading deformation sequences, Thin-Walled Structures 209 (2025) 112879. https://doi.org/10.1016/J.TWS.2024.112879.

[14] T. Frenzel, C. Findeisen, M. Kadic, P. Gumbsch, M. Wegener, Tailored buckling mcrolattices as reusable light-weight shock absorbers, Advanced Materials 28 (2016) 5865–5870. https://doi.org/10.1002/adma.201600610.

[15] S. Tan, D. Pan, Z. Wu, Multi-stable metastructure with multi-layer and multi-degree of freedom: A numerical and experimental investigation, Mater Des 240 (2024). https://doi.org/10.1016/j.matdes.2024.112859.

[16] N. Kidambi, R.L. Harne, K.W. Wang, Energy capture and storage in asymmetrically multistable modular structures inspired by skeletal muscle, Smart Mater Struct 26 (2017) 1–15. https://doi.org/10.1088/1361-665X/aa721a.

[17] M. Alturki, R. Burgueño, Multistable cosine-curved dome system for elastic energy dissipation, J Appl Mech 86 (2019) 091002. https://doi.org/10.1115/1.4043792.

[18] P.K. Mallick, Fiber-Reinforced Composites, CRC Press, 2007. https://doi.org/10.1201/9781420005981.

[19] J.G. Häberlee, F.L. Matthews, MACRO-INSTABILITY OF UNIDIRECTIONAL CFRP COMPRESSION TEST SPECIMENS, 1994.

[20] M.R. Wisnom, J. Hiiberle, Prediction of buckling and failure of unidirectional carbon fibre/epoxy struts, 1994.

[21] R. Fangtao, X. Chenglong, W. He, W. Hongjie, Z. Hongmei, X. Zhenzhen, Experimental study on axial compressive properties and failure mechanism of unidirectional covered carbon fiber-reinforced polymer composites, Polymers and Polymer Composites 30 (2022). https://doi.org/10.1177/09673911221129088.

[22] S.P. Timoshenko, J.M. Gere, W. Prager, Theory of Elastic Stability, Second Edition, J Appl Mech 29 (1962). https://doi.org/10.1115/1.3636481.

[23] W., G.R.H., & Z.R.D. [8] McGuire, Matrix structural analysis, 2nd ed., 2000.

[24] Dassault Systèmes, Abaqus user manual, Dassault Systemes, Providence, RI, 2021.

# تأثير نسبالابعاد على حمل الانبعاج للمركبات المقواة بألياف الكربون أحادية الاتجاه

**الملخص**: تعمل حالات عدم الاستقرار المرنة، مثل الانبعاج والفرقعة، كآليات رئيسية في المواد الفوقية والهياكل الدورية المصممة للتمركز الذاتي وامتصاص وتبديد الطاقة. تعتمد هذه الأنظمة على إحداث انبعاج مفرد أو متعدد لعناصر مترابطة مضغوطة محوريًا. يعتبر مركب الألياف الكربونية' أحادي الاتجاه' مادة واعدة لمثل هذه العناصر، شريطة أن يسبق الانبعاج المرن فشل التلف غير المرن.

تقدم هذه الدراسة تحقيقًا عدديًا لدراسة إجهاد الفشل لمركبات الألياف الكربونية أحادية الاتجاه بنسب أبعاد (AR) مختلفة. أُجريت تحليلات العناصر المحدودة على عينات مختبرة من مركبات بوليمر مقوى بألياف الكربون أحادية الاتجاه موجودة في الأدبيات. تشير النتائج إلى أن الحد الأدنى لنسبة الأبعاد يبلغ 28 ضروريًا لتحفيز فشل الانبعاج بدلًا من الأنماط الأخرى، مع قدرة معادلة أويلر على التنبؤ الكافي بإجهاد الانبعاج الحرج في هذا النطاق. من ناحية أخرى، بالنسبة لقيم نسبة الأبعاد بين 15 و 28، يصبح فشل القص الانضغاطي أو القص مهيمنًا، بينما تؤدي نسبة الأبعاد الأقل من 15 عادةً إلى فشل الانضغاط. إن أخذ تصحيح القص واللاخطية المادية في الاعتبار يمكّن من التنبؤ الدقيق بإجهاد الانبعاج الحرج عبر جميع نسب الأبعاد.